A general approach for studying the motion of a cantilever beam interacting with a 2D fluid flow

Riccardo Baudille and Marco Evangelos Biancolini*

*Department of Mechanical Engineering University of Rome "Tor Vergata",
Via del Politecnico 1, 00133 Roma, Italy*

Abstract. In this paper a general approach for studying the motion of a cantilever beam interacting with a 2D fluid flow is presented. The fluid is solved by a general purpose commercial computational fluid dynamics (CFD) package (FLUENT 6.2), while the structure is managed by means of a dedicated finite element method solver, coded in FLUENT as a user-defined function (UDF). A weak fluid structure interaction coupling scheme is adopted exchanging information at the end of each time step. An arbitrary cantilever beam can be introduced in the CFD mesh with its wetted boundaries specified; the cantilever can also interact with specified rigid and flexible walls through use of a non-linear contact algorithm. After a brief review of relevant scientific contributions, some test cases and application examples are presented.

Keywords: cantilever beam; computational fluid dynamics; finite element methods; fluid-structure interaction; weak coupling.

1. Introduction

Fluid-structure interaction (FSI) is a very interesting topic and it is the key for resolving many physical problems that cannot be handled separately from a structural or a fluid point of view. However, integrated solution of both problems is a difficult challenge, especially in the numerical modelling of strong non linear problems where advanced solution strategies and tools are available only for separate problems. In such cases, it is the interaction between the fluid and adjoining structure that governs the physical behaviour of the entire system. In fact, some coupled problems can converge in a stable configuration, others can generate an oscillating solution, and some others can produce an unstable behaviour.

With focus on the FSI general solution strategies, a brief review of relevant scientific contributions of the last decade is conducted. Genevaux and Bernardin (1996) presented an FSI application adopting a multibody technique for the structural solution, by subdividing a beam in rigid bodies connected by elastic joint, and a kinetic gas-lattice method for the solution of the flow field. Two cases were presented, i.e., the fluid motion induced by the movement of the structure and the structural deformation induced by the flow field. Wall and Ramm (1998) gave a deep insight

---

* Corresponding Author, E-mail: biancolini@ing.uniroma2.it

about theoretical topics of FSI, in which 2D finite element method (FEM) solvers were presented both for the fluid and structure, adopting a weak coupling, i.e., a time marching solution in which the structure and fluid were solved separately and exchange information at the end of each time step. Two practical applications were proposed, i.e., the flow in a channel with a flexible boundary, suitable for the blood motion analysis, and the vortex shedding produced by a cantilever beam in the stream of a bluff body.

Further studies along these lines were carried out by Hübner *et al.* (2002, 2004) and Wall and Ramm (2004). In the work by Hübner *et al.* (2002), a strong coupling was presented with a FEM monolithic strong coupled solver developed by the authors. Both problems were formulated and solved simultaneously at each time step. Non linear Lagrangian motion was considered for the structural part, while a mixed Lagrangian Eulerian technique was implemented for the fluid. Several applications were presented, including the vortex shedding of the cantilever beam.

Kölke *et al.* (2004) presented a strongly coupled numerical analysis of FSI with two immiscible fluid flows using a discretization method based on stabilized space-time finite elements. Numerical results for the collapse of a water column onto an elastic dam were compared with experimental data in order to validate the numerical method. Kämpchen *et al.* (2004) presented both numerical and experimental results for a wing interacting with a flow field. The 3D motion of the wing was solved by a FEM approach using beam elements of the Timoshenko theory. The fluid motion was solved by a 3D computational fluid dynamics (CFD) solver based on the Euler or Navier-Stokes equations, depending on the flux intensity. Strong coupling technique was adopted. In the work by Hübner *et al.* (2004), the problem of vortex shedding was revisited with a strong coupled non linear solver, showing how different stable periodic solutions can arise if different initial conditions are imposed.

A paper devoted to the general problem of shell structures design in civil and mechanical engineering was presented by Wall and Ramm (2004). Also FSI topics were covered including the vortex shedding of a cantilever, modelled by beam elements, and the study of a channel with an internal obstacle represented by a flexible cylindrical shell. Matthies and Steindorf (2003) presented a theoretical study of FSI with the main advantages and disadvantages of weak and strong coupling FSI solvers discussed. Furthermore, a strong approach was proposed, based on a numerical evaluation of the Jacobian of the complete system of equations obtained by separate solvers. Such an approach offers a great reduction in time step, but the numerical effort required for differentiation leads to similar computation performance.

Jahromi *et al.* (2008) recently have published a contribution about nonlinear soil-structure interaction using an iterative coupling technique. After a review about solution strategies for coupled problem comparing monolithic and coupled solvers, several coupling strategies for the weak approach were presented discussing their numerical performances.

The FSI capability was included by multiphysics FEMLab solver COMSOL (2004) for a cantilever beam subjected to a transversal flow, in which a progressive deflection was observed followed by a sudden release with a vortex generation. Tarnopolsky *et al.* (2000) proposed an experimental study on the vortex structures generated by reed petals movement of the wind instruments. This work indicates that the vortexes are produced mainly by the motion of the petal, which is not particularly influenced by the fluid dynamics. A FLUENT simulation was also proposed in this work, where the petal was modelled as a non flexible structure with a rigid motion, for the sake of analysing the vortex structures produced.

A theoretical solution for the flags excited by variable direction winds was given by Fitt and Pope

(2001) considering the potential flow field and beam theory. Chang and Moretti (2002) investigated the problem of tensioned sheet flutter related to papermaking industry using the plate theory and potential flow field. A similar approach was followed by Tang *et al.* (2003) in experiments of the flutter motion for a thin plate mounted downstream to a NACA airfoil, together with numerical analysis based on the potential flow and non linear beam theory. Vairo (2003) presented a study for the evaluation of wind loads around the girder of a long span bridge. In this work, a detailed CFD solution in 2D was performed by the ALE scheme for the stationary cases and for the time histories of cross section movements. Mollendorf *et al.* (2003) presented a theoretical study for the prediction of the movement of a slender body immersed in a fluid. The investigation of the movement of a fin during swimming was investigated, indicating a close agreement between experiments and numerical results. Stein *et al.* (2003) presented a study about aerodynamic interactions between parachute canopies. In the first part the critical distance of interaction between rigid canopies was evaluated by a finite element formulation for the solution of incompressible Navier-Stokes equation. The effect of structure deformation was then considered by means of a deforming spatial domain / stabilized space time finite element formulation.

In this paper an FSI approach is presented for a cantilever beam interacting with a surrounding two dimensional flow field. A detailed description of the practical aspect of implementation was given by Baudille and Biancolini (2005). The structural dynamic problem is very simple, but it is also a good starting point for studying the FSI problems. In fact, it is possible to simulate several practical applications, such as the reed valves opening, flag motion, paper sheet motion in paper making, horizontal motion of skyscrapers interacting with wind, interaction between dams and water waves. It is worthy to notice that the described problem involves a simple structure (cantilever beam) interacting with a complex flow field, which can be turbulent, multiphase or other multi-physics materials. For this reason, the FSI model has been developed for the general purpose CFD solver FLUENT. A dedicated FEM solver for the cantilever evolution has been coded as a user-defined function (UDF). Arbitrary Euler beams are handled by the model with the non-linear effects included, such as the contact between rigid and flexible walls.

In order to test the accuracy of the proposed method, a benchmark test is first conducted by investigating the reference cases proposed by Wall and Ramm (1998) and Hübner *et al.* (2002). More complex applications are studied through solution of the problem of a water wave interacting with a flexible dam proposed by Kölke *et al.* (2004). Finally, the practical application of a reed valve for two strokes combustion engines proposed by Fleck *et al.* (1987) is investigated.

2. Theoretical background

As previously mentioned, this work is focused on a simple geometry, a cantilever beam in planar motion (Fig. 1). Beam theory is applicable for all the structures in which the extension in the longitudinal direction is larger than the extension in the lateral directions. In this case, the structure can be represented by a curve, with the curvilinear abscissa, and the local shape of the cross section at each point along the curve. For the special case where the curve belongs to a plane and the cross section is symmetric with respect to this plane, along with boundary conditions and loads that are symmetric, the beam undergoes a planar motion in the symmetry plane. For the present purposes, we shall assume that the width of the cross section of the beam is constant, but the thickness is a variable along the curve.
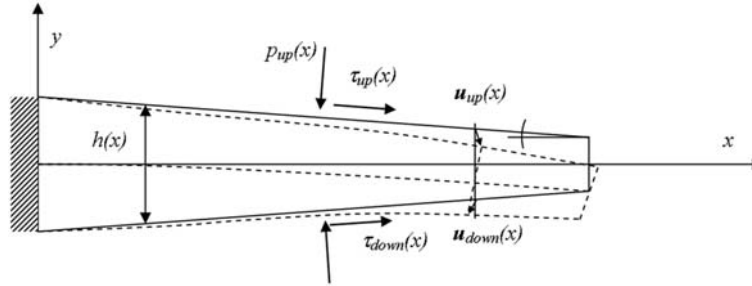
Fig. 1 Cantilever beam

The aforementioned problem can be solved on the structural point at two different levels of detail. One way is to consider the planar problem with the hypothesis of plane strain or plain stress using the continuum mechanics principles. This approach is general and powerful, because no restrictions on the shape of the structure are required. Furthermore, it allows us to deal with the structural part with the same dimensionality used for the surrounding fluid field representation. The main disadvantage is that thin structures are difficult to handle, because a very fine discretization is required for the numerical solution in order to preserve a regular grid dimension in the cross section and along the beam. The other way is to adopt the beam theory by which a solution for the through-the-thickness displacement field can be obtained with the global motion given at the level of curvature-bending dual variables, rather than at the local stress-strain field. The latter is the approach to be adopted in this study.

Under the hypothesis of small displacements for a straight member, the following curvature-bending relation holds:

$$M(x) = EI(x)\chi \cong EI(x)\frac{\partial^2 v_0}{\partial x^2} \tag{1}$$

where E is the material Young modulus, χ is the curvature (that can be approximated by the second derivative of the transversal displacement v_0 along the beam direction x) and $I(x)$ is the cross section moment of inertia that for the constant width w beam with variable thickness t given as

$$I(x) = \frac{w \cdot t(x)^3}{12} \tag{2}$$

The motion of the beam is governed by the following differential equation:

$$-\frac{\partial}{\partial x^2}\left[EI(x)\frac{\partial^2 v_0(x, t)}{\partial x^2}\right] + f(x, t) = m(x)\frac{\partial^2 v_0(x, t)}{\partial t^2} \tag{3}$$

where $m(x)$ is the mass/length of the cross section, $f(x,t)$ is the transversal applied load, and t is time.

The boundary conditions are imposed for the lateral displacement and its derivatives for the beam. For a cantilever, zero displacement and rotation are imposed at the clamped end ($x = 0$), and zero bending moment and transversal force are imposed at the free end ($x = L$), that is,

$$v_0(0, t) = 0, \qquad \frac{\partial v_0(0, t)}{\partial x} = 0 \tag{4}$$

$$EI(L)\frac{\partial^2 v_0(L, t)}{\partial x^2} = 0, \qquad \frac{\partial}{\partial x}\left[EI(L)\frac{\partial^2 v_0(L, t)}{\partial x^2} \right] = 0 \tag{5}$$

For a very thin structure where a zero thickness internal boundary is considered in the fluid, the displacement field given by the classical beam theory is applicable, which can be expressed in terms of the deformed shape of the middle line, considering the out of plane displacement and its derivatives. For a finite-thickness structure, an accurate representation of the displacements field is required in order to properly trace the movement of the interface between the structure and fluid domains.

Considering the complete displacement field of the beam (that is the one to be used in the fluid coupled calculation):

$$u(x, y) = -y \cdot \frac{\partial v_0(x)}{\partial x}$$

$$v(x, y) = v_0(x) \tag{6}$$

the following functions are valid at upper and lower faces of the beam:

$$u_{up}(x) = \frac{t(x)}{2} \cdot \frac{\partial v_0(x)}{\partial x}, \qquad u_{down}(x) = -\frac{t(x)}{2} \cdot \frac{\partial v_0(x)}{\partial x}$$

$$v_{up}(x) = v_0(x) \qquad v_{down}(x) = v_0(x) \tag{7}$$

At the interfaces, the fluid interacts with the structure by means of pressure forces ($p_{up}(x)$ and $p_{down}(x)$) and shear forces ($\tau_{up}(x)$ and $\tau_{down}(x)$). By the hypothesis of small displacement, the effect of shear forces produced by friction at the boundary layer can be neglected, because it produces mainly horizontal loads which affect only the axial deformation of the structure. The transversal applied load is given by the following expression:

$$f(x, t) = w(p_{up}(x) - p_{down}(x)) \tag{8}$$

However, for the case of tapered beams, the friction can also introduce a transversal component that has to be accounted for. If this is the case, the resultant of pressure forces in the transversal direction has to be considered as well,

$$f(x, t) = w(p_{up}\cos\alpha(x) + \tau_{up}\sin(\alpha(x)) - p_{down}\cos(\alpha(x)) - \tau_{down}\sin(\alpha(x))) \tag{9}$$

where the local angle ($\alpha(x)$) can be expressed as the first derivative of the thickness,

$$\alpha(x) = \frac{1}{2}\frac{dt(x)}{dx} \tag{10}$$

3. Numerical model

3.1 Structural model

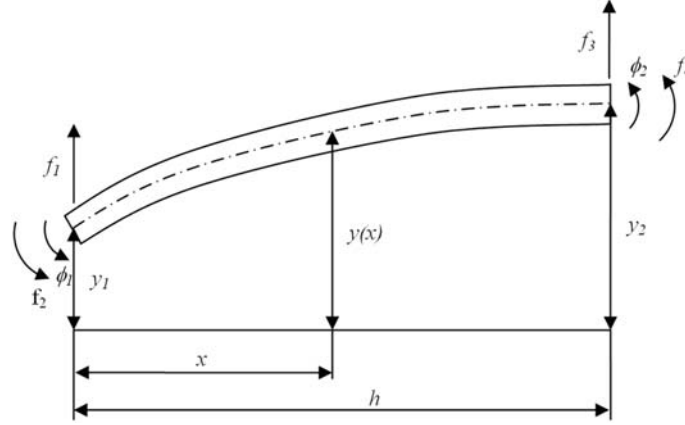Cantilever beam motion was solved by the FEM approach. The element stiffness and mass

Fig. 2 Beam element notation

matrices in closed-form were adopted for the Euler beam theory following the work of Meirovitch (1986). For the 2D beam element shown in Fig. 2, four degrees of freedom are required, i.e., a rotation and an out-of-plane displacement at each node denoted by the vector y:

$$\{y\} = \begin{Bmatrix} y_1 \\ h\phi_1 \\ y_2 \\ h\phi_2 \end{Bmatrix} \tag{11}$$

The force and moment acting on the element are denoted by the vector f:

$$\{f\} = \begin{Bmatrix} f_1 \\ f_2/h \\ f_3 \\ f_4/h \end{Bmatrix} \tag{12}$$

The relation between the forces and displacements of each element is linear:

$$\{f\} = [K_{el}]\{y\} \tag{13}$$

where the stiffness matrix $[K_{el}]$ is

$$[K_{el}] = \frac{EI}{h^3} \begin{bmatrix} 12 & 6 & -12 & 6 \\ 6 & 4 & -6 & 2 \\ -12 & -6 & 12 & -6 \\ 6 & 2 & -6 & 4 \end{bmatrix} \tag{14}$$

The elastic strain energy of the element can be written as

$$E = \frac{1}{2} \{y\}^T [K_{el}] \{y\} \tag{15}$$

The kinetic energy can be written as

$$T = \frac{1}{2} \{\dot{y}\}^T [M_{el}] \{\dot{y}\} \tag{16}$$

where the consistent mass matrix $[M_{el}]$ is

$$[M_{el}] = \frac{mh}{420} \begin{bmatrix} 156 & 22 & 54 & -13 \\ 22 & 4 & 13 & -3 \\ 54 & 13 & 156 & -22 \\ -13 & -3 & -22 & 4 \end{bmatrix} \tag{17}$$

The overall stiffness and mass matrixes are assembled by summing the contributions of all elements at each node of the structure in the global coordinates,

$$[K] = \sum_{i=1}^{N_{dof}} [K_{el}]_i \tag{18}$$

$$[M] = \sum_{i=1}^{N_{dof}} [M_{el}]_i \tag{19}$$

A proportional damping was introduced for the structure in the assembled system as

$$[C] = \frac{2\zeta}{2\pi f_1} [K] \tag{20}$$

The dynamic equation of motion in matrix form can be written as follows:

$$[M]\{\ddot{y}(t)\} + [C]\{\dot{y}(t)\} + [K]\{y(t)\} = \{F(t)\} \tag{21}$$

where $\{F\}$ is the force vector due to external actions. For a complete FSI problem, this vector contains both the structural and fluid forces. The structural forces are produced by the dead weight of the structure itself, which may be given as lumped loads. The fluid forces are produced by the local pressure and shear stress acting on structural faces. The force field on the structural elements is transformed to nodal loads based on energy equivalence.

The Newmark method of central finite difference representation, as exposed by Blakely (1993) for NASTRAN solver, is then adopted for the displacement derivatives for a constant discrete time step:

$$\{\dot{y}\} = \frac{1}{2\Delta t}(y_t - y_{t-2})$$

$$\{\ddot{y}\} = \frac{1}{\Delta t^2}(y_t - 2y_{t-1} + y_{t-2}) \tag{22}$$

With this, the equation of motion (11) can be expressed in discrete form:

$$\{f_{t-1}\} = \left[\frac{M_{tot}}{\Delta t^2}\right](y_t - 2y_{t-1} + y_{t-2}) + \left[\frac{C_{tot}}{2\Delta t}\right](y_t - y_{t-2}) + \left[\frac{K_{tot}}{3}\right](y_t + y_{t-1} + y_{t-2}) \tag{23}$$

After some manipulation, the following time marching scheme can be obtained:

$$\{y_t\} = [A_1]^{-1}[A_2] + [A_1]^{-1}[A_3]\{y_{t-1}\} + [A_1]^{-1}[A_4]\{y_{t-2}\} \tag{24}$$

where each of the matrices is given as

$$[A_1] = \left[\frac{M_{tot}}{\Delta t^2} + \frac{C_{tot}}{2\Delta t} + \frac{K_{tot}}{3}\right]$$

$$[A_2] = \{f_{t-1}\}$$

$$[A_3] = \left[\frac{2M_{tot}}{\Delta t^2} - \frac{K_{tot}}{3}\right]$$

$$[A_4] = \left[-\frac{M_{tot}}{\Delta t^2} + \frac{C_{tot}}{2\Delta t} - \frac{K_{tot}}{3}\right] \tag{25}$$

In the presence of non linear contact forces, the matrix $[A_2]$ is modified as follows:

$$[A_2] = \{f_{t-1}\} - [K_{nonlin}\{y_{t-1} - y_c\}] \tag{26}$$

By so doing, the non linearity contact forces can be handled in an explicit fashion.

3.2 CFD model

The FLUENT commercial CFD code was used to simulate the fluid dynamics evolution. A 2D approach has been chosen to study the phenomena involved. The computational domain is a 2D unstructured mesh composed of triangular elements eventually with consideration for more than one phase. In Fig. 3, a typical mesh for the fluid domain of the vortex shedding benchmark is shown.

The FLUENT can handle a wide range of incompressible and compressible, laminar and turbulent
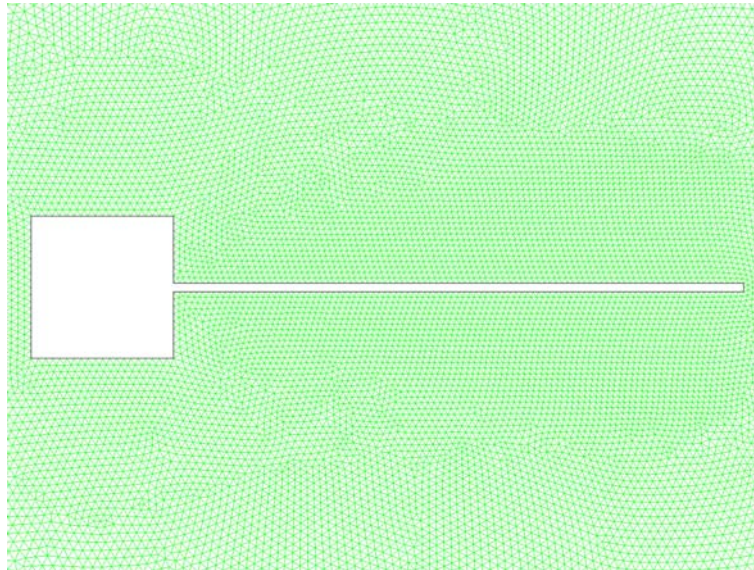

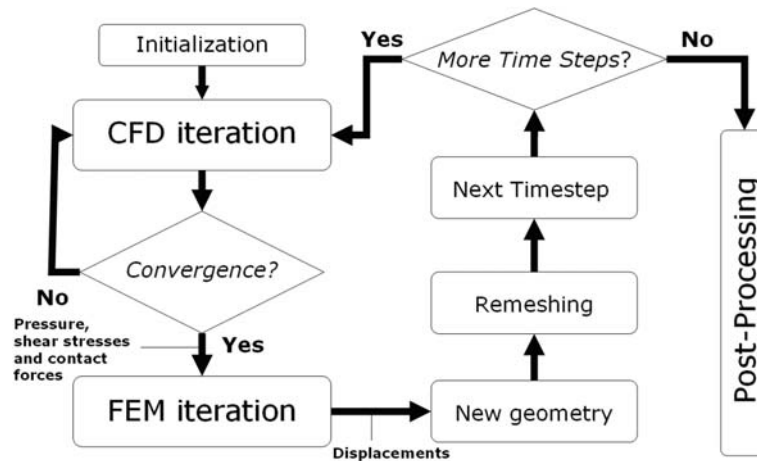Fig. 3 Detail of CFD mesh for the vortex shedding benchmark

Fig. 4 Flow chart of the solution process

fluid flow problems either in steady-state or transient conditions. Moreover, various mathematical models for the transport phenomena, such as heat transfer and chemical reactions, can be taken into account. For all flows, FLUENT solves the conservation equations for mass and momentum using a finite volume discretization technique. For flows involving heat transfer or compressibility, an additional equation for energy conservation is solved. Additional transport equations are also solved when the flow is turbulent. For flows involving mixing or reactions, a special conservation equation is solved. For the case when the non-premixed combustion model is used, conservation equations for the mixture fraction and its variance are also solved.

3.3 CFD/FEM coupling strategy

The coupling technique used is based on a weak approach, in the sense that the structural problem is solved after the fluid time step is made available. The forces applied to the structure are passed by FLUENT at the end of each time step to the FEM solver. Then the structural problem is solved and the new geometry configuration obtained is applied to the fluid domain by means of the moving and deforming (MDM) capability of FLUENT. The flow chart of the solution process is given in Fig. 4. This coupling strategy is very efficient and is capable of handling a wide range of FSI problems. Convergence is ensured by choosing the correct time step size for the coupled problem.

3.4 CFD/FEM interface management

The computational CFD mesh for the fluid domain is prepared as usual with a pre-processing tool. A conformal FEM mesh for the structure is automatically built by the FSI code from the boundary mesh of the fluid domain. Both thin and thick beams are considered. If a zero-thickness structure is modelled in the fluid domain, only two faces of the beam are passed to the FEM solver to build the corresponding beam model. Otherwise, for a non-zero thickness structure, three faces are passed. A basic requirement for the mesh is that the opposite faces of the structure must be aligned and straight in the initial configuration, and that their nodes must be aligned. This condition allows the code to create a line of nodes along the middle line of the structure so as to generate the
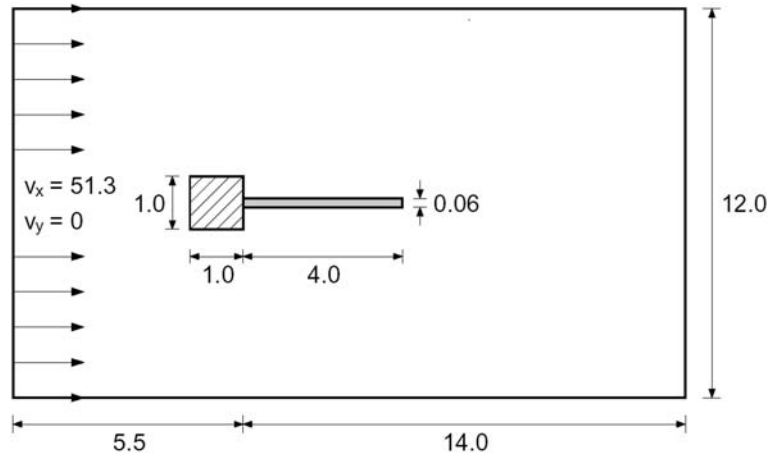
Fig. 5 Geometry of the test case

beam elements between them. For a non-zero thickness cantilever, not only the vertical displacements, but also the rotations of the section are taken into account in order to correctly move the CFD boundary nodes. Furthermore, a coordinate system transformation is implemented for describing the general position and orientation of the cantilever and for transforming all information from the global coordinate system to the local one.

4. Cases of study

4.1 Vortex shedding

A well-known benchmark problem has been used as an initial test of the present approach, i.e., the vortex shedding excitation of a cantilever beam positioned downstream of a square obstacle in a laminar flow. From a structural point of view, the deformed shape of the cantilever is determined by the pressure load and shear stresses. From a fluid dynamics point of view, the beam constitutes a time-varying boundary condition for the fluid flow. The reference results for the benchmark were available in the works by Wall and Ramm (1998) and Hübner *et al.* (2002). The geometry of the problem is given in Fig. 5, where all dimensions are expressed in metres.

The fluid has a density of $1.18 \ 10^{-3} \ \text{kg/m}^3$ and a viscosity of $1.82 \ 10^{-4} \ \text{Pa} \cdot \text{s}$. The structure is characterized by a density of $0.1 \ \text{kg/m}^3$ and a Young's modulus of $2.5 \ 10^6$ Pa. The boundary conditions of the test case are a velocity inlet of 51.3 m/s, a constant outlet static pressure, a free sleep condition on the lateral walls, and a no-slip condition on the body and beam walls.

4.2 Breaking dam

A two-phase problem is investigated in order to test the FSI model in combination with other CFD sub-models. A water column is initially placed at the bottom left corner of a tank surrounded by atmospheric air. In the middle of the bottom of the tank, there is a flexible dam. The geometry configuration of the problem is given in Fig. 6 with all dimensions expressed in metres. Under the effect of gravitational acceleration, the water falls down and smashes into the dam, producing its
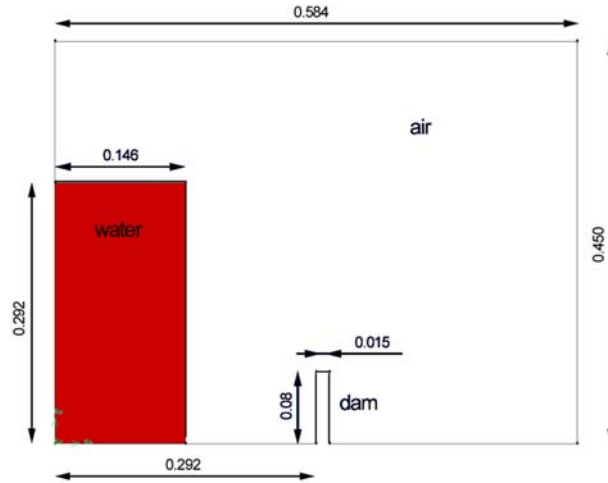
Fig. 6 The initial configuration of the water column and the flexible dam
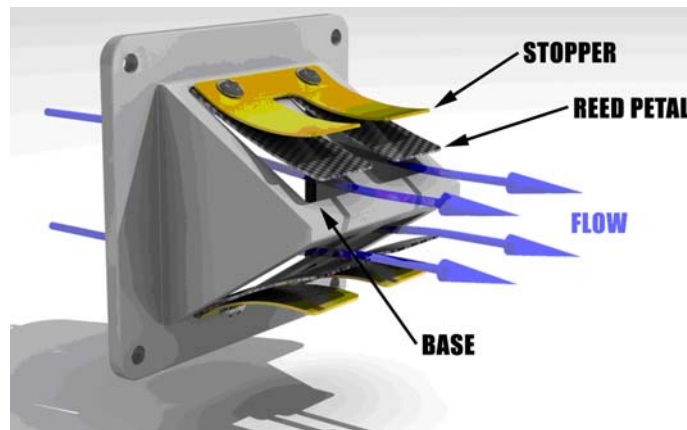

Fig. 7 A diagram of the reed valve, showing the flexible reed petal, base, and stopper

deformation. Free slip boundary condition is applied on all the walls and the top of the tank is considered as an open boundary with a prescribed static pressure condition. The dam is made of rubber with a Young's modulus of 1 MPa and density of 1000 kg/m^3. This case has been studied by Kölke *et al.* (2004), where the time-history responses of the water shapes and dam tip displacements are reported for both the numerical and experimental investigations.

4.3 Reed valve

One practical application that needs an FSI approach is the working cycle of a reed valve. Reed valves are pressure-driven flow stoppers, used in systems such as two-stroke engines, compressors and shock absorbers. A typical reed valve configuration is shown in Fig. 7. The reed petal is made of flexible material and mounted between a base and a stopper. The base serves as a barrier for valve closure, while the upper stoper, which can be curved, has a double function: it serves as a guide to prevent excessive opening of the valve, while optimising the shape of the open channel

Table 1 Yamaha RD350 engine characteristics

Model	Yamaha RD 350 LC
Swept volume	347 cm^3
Cylinders	2
Bore	64 mm
Stroke	54 mm
Connecting rod length	110 mm
Trapped compression ratio	6 : 1
Reed valve arrangement	V-block
Number of reed petals	4
Carburettor diameter	26 mm

Table 2 characteristics of the reed petal analysed

Material	Glass fibre
Density	1850 Kg/m^3
Young's modulus	$21.5 \cdot 10^9$ Pa
Free length	29.0 mm
Width	22.0 mm
Thickness	0.46 mm
Stopper radius	48.0 mm

from a fluid dynamics point of view.

The overall gas dynamics and local fluid motion depend on the open area of the valve. The open area in turn depends on the reed motion, which is driven by pressure loads produced by the fluid. Air suction in the crankcase is produced when the piston moves toward top dead centre (TDC). This gives rise to a pressure difference relative to the inlet manifold, which causes the reed valve to open. The actual behaviour is complicated by the valve dynamics, the inertial effects of the entering air, and a local vortex.

Baudille and Biancolini (2002) have studied the non linear dynamics of this component by lumping the effects produced by the fluid motion as an equivalent viscous load. In the present work, an FSI simulation was performed for the reed valve of the Yamaha RD350 engine studied by Fleck *et al.* (1987). The main engine characteristics are reported in Table 1. The reed petal analysed in this work is made of fibreglass with the major characteristics listed in Table 2. The reed valve has been modelled as a 2D problem. By taking into account the symmetry condition with respect to the middle line of the valve, only half of the engine manifold is modelled. Actual pressure histories found in this work were applied as boundary conditions at the inlet and outlet boundaries of the CFD domain. The applied pressure difference will be shown in the results section.

5. Results

5.1 Vortex shedding

In order to quickly achieve the expected solution of stationary vortex shedding, a steady
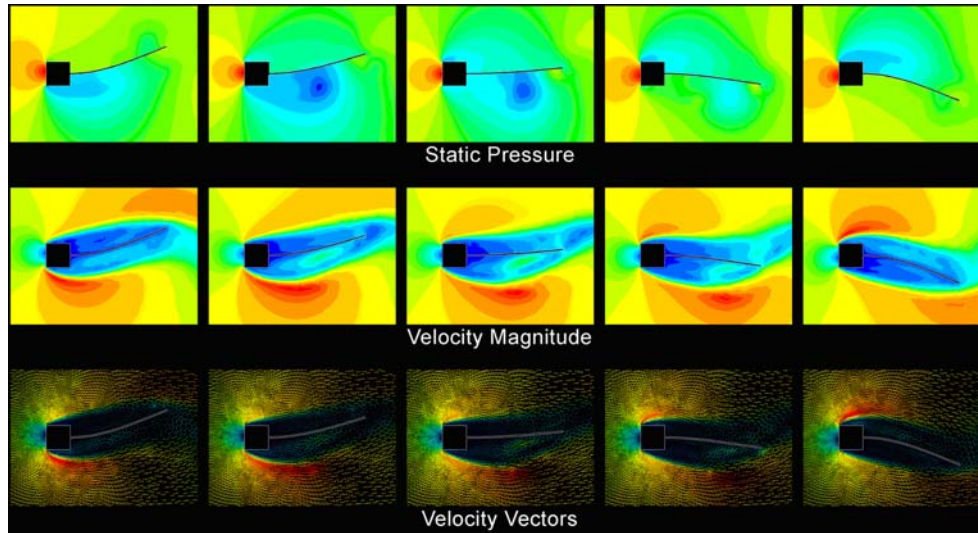
Fig. 8 Simulated pressure and velocity fields around the square bluff body and the slender flexible structure for different times
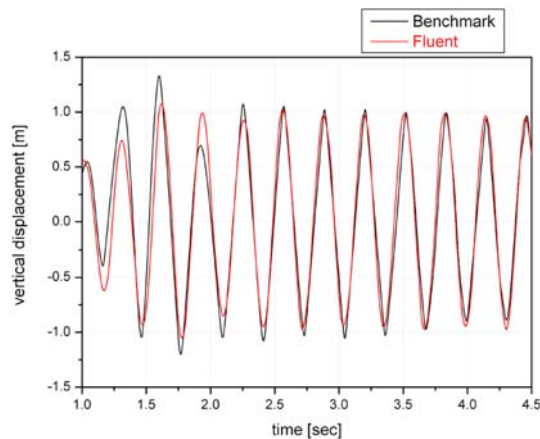

Fig. 9 Vertical displacement of the beam free end predicted by the FSI model compared to literature reference data by Wall and Ramm (1998) and Hübner *et al*. (2002)

calculation of five hundred iterations was first performed without the FSI model. The flow field obtained was then applied as the initial condition for the unsteady FSI simulation. This procedure shortens the total calculation time, but does not affect the final result.

The fluid dynamics problem is laminar, given a Reynolds number of 333. The vortex shedding frequency of the isolated square cylinder is 6.25 Hz, corresponding to a Strouhal number of 0.12, while the first natural frequency of the cantilever beam is 3.03 Hz. Comparing these frequencies to the resulting frequency of the coupled problem of 3.18 Hz, we can conclude that the coupled behaviour is dominated by the first mode of the cantilever beam. Animations of the CFD predictions for the pressure and velocity fields around the bluff body and the slender flexible structure are consistent with expectations, as shown in Fig. 8. The result obtained for the vertical displacement of the free end of the beam with respect to time is in good agreement with the reference cited above, as illustrated in Fig. 9.

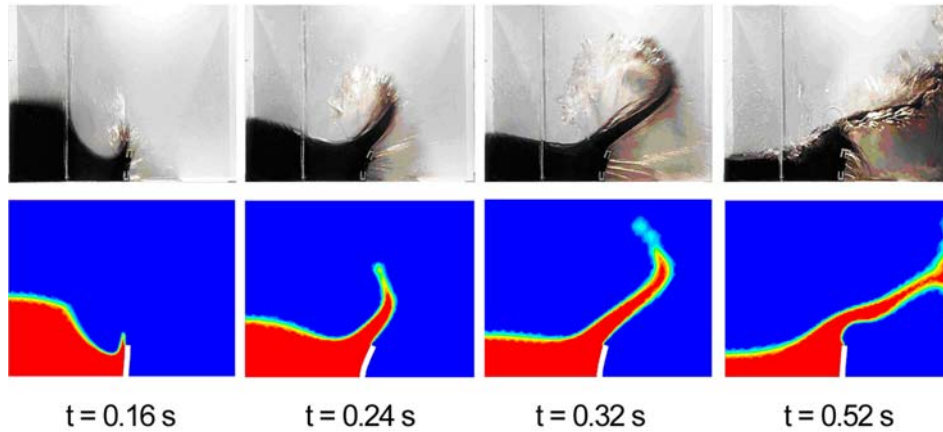t = 0.16 s   t = 0.24 s   t = 0.32 s   t = 0.52 s

Fig. 10 Comparison of the water shape between experimentation and simulation
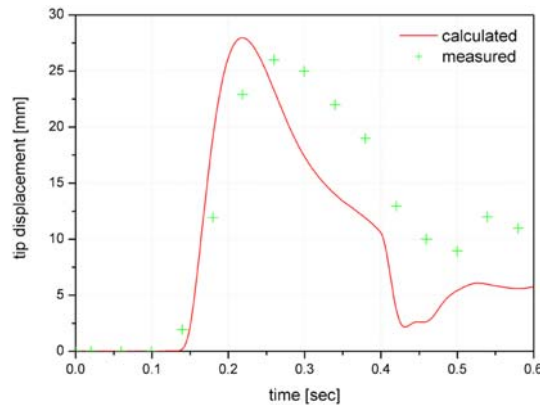

Fig. 11 Horizontal tip displacement of the dam predicted by the FSI model and measured experimentally by Kölke *et al.* (2004)

5.2 Breaking dam

The two-phase problem of the breaking dam was simulated by the FLUENT multiphase model Volume Of Fluid (VOF), with the Geo-Reconstruct scheme, in conjunction with the proposed FSI model. The air fluid was considered as a compressible ideal gas, because its compressibility plays a crucial role when the air is trapped by water in a closed volume, as shown in the simulation results. Both the surface tension and wall adhesion of water are neglected. The FLUENT standard k-e turbulence model has been used for the fluid dynamics simulation.

Initially the water column begins to fall down and then it reaches the obstacle which starts to be deformed by the water mass impact. During the raise of water on the left side of the dam, the deformation of the structure increases until it reaches the maximum when the water has flown more than one dam length over the tip. Then the tip displacement starts to decrease, showing a sudden reduction when the water impinges on the right wall of the tank. Subsequently, some tip oscillation are observed, when the water starts to cover all the free end of the structure.

Fig. 10 shows a comparison of the water shape between the experimental images and simulation contours. In Fig. 11 the horizontal displacement of the free end of the dam is plotted versus time,
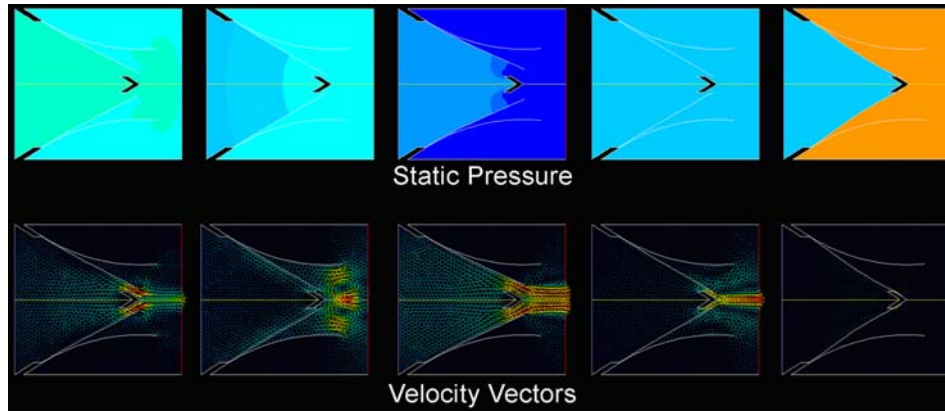
Fig. 12 Flow fields in the reed valve at various times during an engine cycle at 4770 RPM
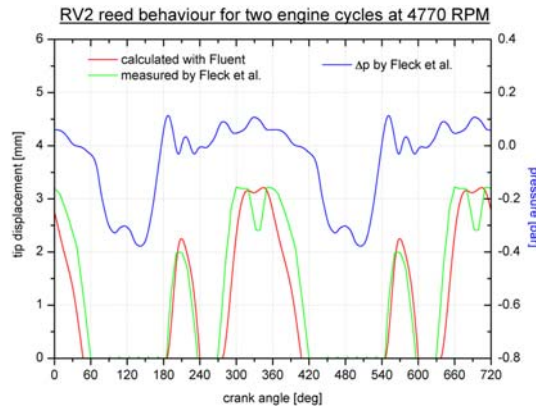

Fig. 13 Tip displacement of the reed valve predicted by the FSI model and measured experimentally by Fleck *et al*. (1987); the measured pressure differential is also shown

both for numerical and experimental data. All experimental reference data are taken from the results by Kölke *et al*. (2004). It is confirmed that good agreement has been made between the present results and experiment ones. A little lack of accuracy can be attributed to some simplifications that have been made. For instance, the simulated case is two-dimensional, but the real structure is three-dimensional. The dam is modelled as a cantilever beam with its elasticity taken as linear. However, the actual rubber behaviour is far from this. Finally, the small displacements approach has been used, even though the deformation of the structure is not small.

5.3 Reed valve

Numerical simulation results of the reed valve described above is illustrated in this paragraph. The FSI model was used here with the contact algorithm capability, in order to correctly simulate the contact of the petal with its stoppers. The FLUENT standard k-ε was chosen as turbulence model for the fluid simulation.

The pressure and velocity fields are illustrated in Fig. 12 for various time steps for an engine cycle at 4770 RPM. From these images, one may notice the reed petal reaction to the pressure

variation, the vortex formation downstream the valve, and the predicted bouncing of the petal at closure and at full opening by the contact program. The tip vertical displacement of the reed agrees very well with experimental data given by Fleck *et al.* (1987), as shown in Fig. 13.

6. Conclusions

In this paper a dedicated approach for FSI modelling is presented. Structural dynamics was solved by an FEM solver coupled with the commercial CFD solver FLUENT based on a weak coupling approach, i.e., by allowing the information to be exchanged at the end of each time step. The structural model that interacts with the CFD model is defined by specifying the boundaries of deformable parts and contact walls. During the solution, the interface motion is transferred through use of the moving mesh capability of the CFD solver.

In order to validate the code, while illustrating its applicability, three different two-dimensional cases are studied, i.e., the vortex shedding excitation of a cantilever beam positioned downstream of a square obstacle, the interaction between water and a flexible dam, and the working cycle of a reed valve. It is interesting to note that the complexity of applications is increased through the examples. In the vortex shedding test, the cantilever interacts with a single phase laminar fluid. As for the case of a breaking dam, a two phase fluid is required for tracking the interface between air and water. In the reed valve test, the problem is further complicated by the contact interaction between the reed and stopper.

For all the applications satisfactory results in term of the dynamics behaviour of coupled structures have been obtained, as indicated by the close agreement with reference results. It is confirmed that, despite its simplicity, the proposed solution scheme can be considered a versatile and robust approach for the solution of FSI problems.

References

Baudille, R. and Biancolini, M. E. (2002), "Dynamic analysis of a two stroke engine reed valve", *Proceedings on CD-ROM of XXXI AIAS Conference*, Parma, Italy. (available on-line in Italian http://www.pcm.unifi.it/Aias/ XXXI_CONVEGNO/CD_ATTI/PDF/149.pdf).

Baudille, R. and Biancolini, M. E. (2005), "Modelling FSI problems in FLUENT: a dedicated approach by means of UDF programming", *Proceedings on CD-ROM of the European Automotive CFD Conference*, Frankfurt, Germany.

Blakely, K. (1993), MSC/Nastran v68 Basic Dynamic Analysis guide. MSC Corp.

Chang, Y. B. and Moretti, P. M. (2002), "Flow-induced vibration of free edges of thin films", *J. Fluids Struct.*, **16**(7), 989-1008.

Comsol Inc., "Fluid-structure interaction example of multiphisics application", Femlab internet site, 2004.

Fitt, A. D. and Pope, M. P. (2001), "The unsteady motion of two-dimensional flags with bending stiffness", *J. Eng. Mathematics*, **40**(3), 227-248.

Fleck, R., Blair, G. P. and Houston, R. A. R. (1987), "An improved model for predicting reed valve behaviour in two-stroke cycle engines", SAE Paper no. 871654.

Genevaux, J. M. and Bernardin, D. (1996), "The lattice gas method and interaction with an elastic solid", *J. Fluids Struct.*, **10**, 873-892.

Hübner, B., Walhorn, E. and Dinkler, D. (2002), "Space-time finite elements for fluid-structure interaction", *Proceedings in Applied Mathematics and Mechanics*, **1**(1), 81-82.

Hübner, B., Walhorn, E. and Dinkler, D. (2004), "A monolithic approach to fluid-structure interaction using space-time finite elements", *Comput. Methods Appl. Mech. Eng.*, **193**, 2087-2104.

Jahromi, H. Z., Izzuddin, B. A. and Zdravkovic, L. (2008), "Partitioned analysis of nonlinear soil-structure interaction using iterative coupling", *Interaction and Multiscale Mechanics, An Int. J.*, **1**(1), 33-51.

Kämpchen, M., Dafnis, A., Reimerdes, H. G., Britten, G. and Ballmann, J. (2004), "Dynamic aero-structural response of an elastic wing model", *J. Fluids Struct.*, **18**, 63-77.

Kölke, A., Hübner, B., Walhorn, E. and Dinkler, D. (2004), "Strongly coupled analysis of fluid-structure interaction with two-fluid flows", *Proceedings on CD-ROM of the European Congress on Computational Methods in Applied Sciences and Engineering, ECCOMAS 2004*, Jyväskylä, Finland. (available on-line http://www.mit.jyu.fi/eccomas2004/proceedings/pdf/28.pdf).

Matthies, H. G. and Steindorf, J. (2003), "Partitioned strong coupling algorithms for fluid-structure-interaction", *Comput. Struct.*, **81**(8-11), 805-812.

Meirovitch, L. (1986), *Elements of Vibration Analysis*, McGraw Hill, New York.

Mollendorf, J. C., Felske, J. D., Samimy, S. and Pendergast, D. R. (2003), "A fluid/solid model for predicting slender body deflection in a moving fluid", *J. Appl. Mech.*, **70**(1), 346-350.

Stein, K., Tezduyar, T., Kumar, V., Sathe, S., Benney, R., Thornburg, E., Kyle, C. and Nonoshita, T. (2003), "Aerodynamic interactions between parachute canopies", *J. Appl. Mech.*, **70**(1), 50-57.

Tang, D. M., Yamamoto, H., H. Dowell, E. (2003), "Flutter and limit cycle oscillations of two-dimensional panels in three-dimensional axial flow", *J. Fluids Struct.*, **17**(2) 225-242.

Tarnopolsky, A. Z., Fletcher, N. H. and Lai, J. C. S. (2000), "Oscillating reed valves-an experimental study", *J. Acoustical Society of America*, **108**(1), 400-406.

Vairo, G. (2003), "A numerical model for wind loads simulation on long-span bridges", *Simulation Modelling Practice & Theory*, **11**(5-6), 315-351.

Wall, W. A. and Ramm, E. (1998), "Fluid-structure interaction based upon a stabilized (ALE) finite element method in computational mechanics - New trends and applications", *Proceedings on CD-ROM of the 4th World Congress on Computational Mechanics (WCCM IV)*, Idelsohn SR, Oñate E, Dvorkin EN (eds) CIMNE, Barcelona.

Wall, W. A. and Ramm, E. (2004), "Shell structures - a sensitive interrelation between physics and numerics", *Int. J. Numer. Methods Eng.*, **60**, 381-427.